

Document downloaded from:

<http://hdl.handle.net/10251/154386>

This paper must be cited as:

Cabrera Marcet, E.; Del Teso-March, R.; Gomez Selles, E.; Estruch-Juan, ME.; Soriano Olivares, J. (2019). Quick energy assessment of irrigation water transport systems. *Biosystems Engineering*. 188:96-105. <https://doi.org/10.1016/j.biosystemseng.2019.10.013>



The final publication is available at

<https://doi.org/10.1016/j.biosystemseng.2019.10.013>

Copyright Elsevier

Additional Information

QUICK ENERGY ASSESSMENT OF IRRIGATION WATER TRANSPORT SYSTEMS

Cabrera E., del Teso R., Gómez E., Estruch E. and Soriano J.

ABSTRACT

Pressurised water transport systems are highly energy-intensive. Therefore, in the context of resource scarcity and climate change, efficiency is essential. To achieve this, it is necessary to (1) assess the state of the process and (2) evaluate the existing margin for potential improvement. These are the two objectives of this work, which is based on the energy intensity I_e (kW h m^{-3}) of a process that can simultaneously be expressed in units of pressure. Considering water transport, and its incompressible behaviour, there exists a biunivocal relationship between I_e and the sum of energy required to transport water, which can be expressed as equivalent height H (m, energy per unit of mass). From the energy intensity (I_e) and energy requirements (H), the efficiency of a water transport system in operation is evaluated. From installations in the design phase, the range of I_e values that are needed to achieve efficiency can be predicted. The proposed procedure is general, simple and precise, as demonstrated through three case studies.

Nomenclature

Symbols	Meaning of symbols
$a_o(p)$	Constant, depending on working pressure and material cost of the pipe [$\text{€ (m m}^2\text{)}^{-1}$]
c	Adjustment exponent of material cost evolution
C_I	Energy source context indicator [kW h]
E_I	Supplied (or injected) energy [kW h]
E_N	Natural energy [kW h]
E_p	Shaft (pumping) energy [kW h]
E_{si}	Minimum energy required by the system [kW h]
E_{ti}	Topographic energy [kW h]
f	Friction factor
F_i	Installation factor
f_p	Investment - installation - construction factor
H	Piezometric head [m]
h	Number of operating hours [h year^{-1}]
H_d	Designed height [m]
h_f	Pressure losses [m]
η_{GL}	Global efficiency [%]
H_{PAT}	Energy to be recovered by the PAT [kW h]
I_e	Energy intensity [kW h m^{-3}]
J_{max}	Maximum hydraulic slope [m km^{-1}]
J_{min}	Minimum hydraulic slope [m km^{-1}]
J_o	Optimal hydraulic slope/gradient [m km^{-1}]
J_o^*	Optimal slope of a gravity pipe [m km^{-1}]

L	System length [m]
L_{ei}	Equivalent lengths of the accessories [m]
$\overline{p_e}$	Global average price of energy [€ (kW h) ⁻¹]
$\overline{p_e}^*$	Average selling energy price [€ (kW h) ⁻¹]
p_i	Pressure at the origin [N m ⁻²]
p_o	Service pressure [N m ⁻²]
Q	Flow [m ³ s ⁻¹]
v_j	Water consumption of node j [m ³]
w_f	Friction efficiency
\bar{z}	Weighted average of the consumption nodes [m]
z_f	Final node elevation [m]
z_h	Elevation of the highest node [m]
z_i	Initial node elevation [m]
z_l	Elevation of the lowest node [m]
γ	Specific weight of water [N m ⁻³]
ΔE	Excess of natural energy [kW h]
η_l	Water efficiency [%]
η_p	Pumping efficiency [%]
θ	Weight of structural losses in the energy balance
λ	Installation cost factor

Abbreviations

<i>PRV</i>	Pressure Reducing Valve
<i>PAT</i>	Pump As Turbine
<i>BEP</i>	Best Efficient Point

17

18 **1. Introduction**

19 The main benefits of pressurised water transport are its flexibility (because its layout is compatible
20 with the topography), water quality conservation (the pipe itself and its internal pressure maintain
21 the water quality) and higher efficiency. That is why there is a general trend towards the
22 transformation of classic irrigation channels into pressurised networks. Its weak point in
23 pressurised water transport is the energy required which is associated with high costs and
24 greenhouse gas emissions. It is, therefore, crucial to minimise the economic and environmental
25 impacts of pressurised water transport that are responsible for a significant percentage of total
26 energy consumption. In Europe, pumps (including those for industrial use) account for 10% of the
27 electricity demand (Grundfoss, 2014), whilst, in California, water transport represents 6% of the
28 total energy demand (WW, 2013). In Spain, pressurised irrigation is responsible for only 3% of
29 the total consumption (Cabrera et al., 2010a). The European Union's reviews of energy-saving
30 objectives are aimed at least an 20% reduction by 2020 (EC, 2011) and 32.5% by 2030 (EC, 2019).
31 Pressurised water transport should contribute to the achievement of these objectives.

32 Improving the performance of an operating pressurised water system requires both the
33 identification of the current system state and the subsequent assessment of the margin for

34 improvement that exists with the current level of available technology. In the design phase of new
 35 systems, energy efficiency must be a fundamental concern. This work synthesises previous
 36 research (Cabrera et al., 2015; Cabrera et al., 2018 and Cabrera et al., 2019) and focuses on their
 37 concepts and presents a quick assessment of the energy efficiency of the reported systems. The
 38 proposed method is accessible to a wide range of professionals.

39 2. Fundamentals of quick energy assessment

40 A simple water transport system consists of movement between two points without any pressure
 41 requirements. The levels and distance between the two points determine the energy requirements.
 42 If the initial elevation, z_i , is lower than the final one, z_f , the system needs shaft (or pumping) energy.
 43 However, if $z_i > z_f$, water can move by gravity, although an additional contribution from pumping
 44 energy may be required to overcome friction, h_f , if it exceeds the available energy (i.e. $h_f > z_i - z_f$).

45 As gravitational energy has no costs, energy analyses have been concentrated on systems with
 46 pumping stations. This restrictive selection is nowadays unacceptable because no form of energy
 47 should be neglected. If a gravitational energy surplus exists, it can be recovered with turbines or
 48 PATs (Pumps as Turbines) reduce energy loss. If that it is not economically feasible, energy can
 49 be dissipated with pressure-reducing valves (PRVs). In other words, efficiency analyses could be
 50 extended to all systems. This work starts with those systems that arouse the most interest (when
 51 pumping is needed) and these are later extended to other cases.

52 The methodology derived here is based on the equivalence between the units of the energy required
 53 to transport 1 m^3 of water, or energy intensity I_e , (kW h m^{-3}), and units of pressure (N m^{-2}). Since
 54 water density is constant, each I_e unit corresponds to pressure height on a 1:1 basis. This
 55 relationship, with $\gamma = 9810 \text{ N m}^{-3}$ in SI units, is

$$I_e \left(\frac{\text{kWh}}{\text{m}^3} \right) = 2.725 \cdot 10^{-3} H(m). \quad (1)$$

56

57 Therefore, $0.2725 \text{ kW h m}^{-3}$ which is equivalent to 100 m of height.

58 However, water transport is not just a matter of its movement and elevation. In networks (and
 59 sometimes in simple systems as well) a specified service pressure, p_o , must be provided. In urban
 60 water networks, this pressure is established by standards (Ghorbanian et al., 2016), whereas, in
 61 irrigation, it is set by the requirements of the devices (e.g. sprinklers or drippers). In short, in ideal
 62 systems, the energy intensity corresponding to the total energy needed (where p_i is the pressure at
 63 the origin) is:

$$I_e \left(\frac{\text{kWh}}{\text{m}^3} \right) = 2.725 \cdot 10^{-3} \left[(z_f - z_l) + \left(\frac{p_o}{\gamma} - \frac{p_i}{\gamma} \right) \right] (m) \quad (2)$$

64 In addition to useful energy, there are also inefficiencies (Cabrera et al., 2015) in pumping stations
 65 and in pipelines (through leaks and friction). There are metrics (η_p and η_l) corresponding to
 66 pumping and water efficiencies. But this is not the case for frictional losses, which, do not allow a
 67 similar concept to be established that defines a relationship between useful and required energy.
 68 Although frictional losses are inevitable, they must be added to energy needs. Thus, Eq. 3 includes
 69 friction, h_f , the sum of all losses in pipes and fittings ($h_f = \sum h_{fi}$). The equivalent height H is therefore

$$I_e \left(\frac{\text{kWh}}{\text{m}^3} \right) = 2.725 \cdot 10^{-3} \left[(z_f - z_l) + \left(\frac{p_o}{\gamma} - \frac{p_i}{\gamma} \right) + \left(\sum h_{fi} \right) \right] \quad (3)$$

70

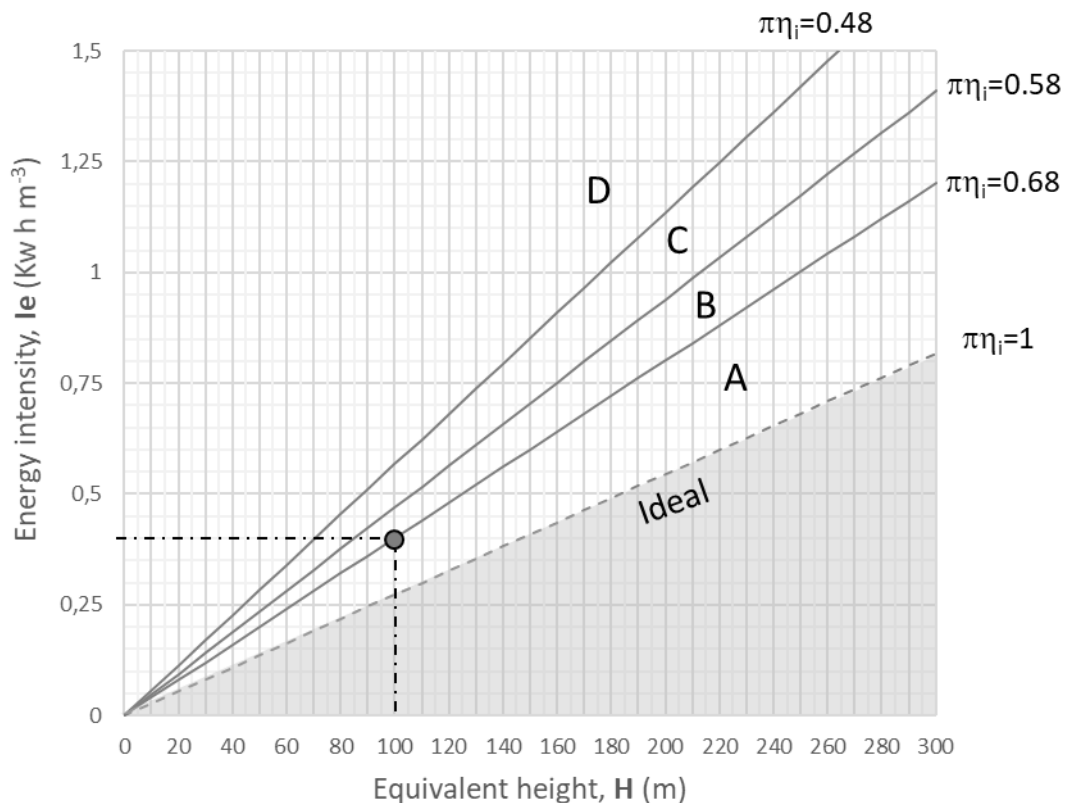
71 The final I_e formula, referred to the delivered volume and including the inefficiencies and the
 72 natural energy ($z_i - z_l$), is

$$I_e \left(\frac{kWh}{m^3} \right) = \frac{2.725 \cdot 10^{-3}}{\eta_p \eta_l} H (m). \quad (4)$$

73 Other inefficiencies (such as the surplus of energy delivered) that are avoidable are not included.

74 Figure 1 graphically depicts Eq. 4 for different efficiency values ($\prod \eta_i = \eta_p \eta_l$), which range from
 75 the ideal case ($\prod \eta_i = 1$) to less efficient systems. To qualify the system's behaviour, in the I_e-H
 76 plane (Fig. 1), four zones are defined: zone A (excellent), zone B (reasonable), zone C
 77 (unsatisfactory) and zone D (unacceptable). The intersection of the horizontal line defined by the
 78 real value of I_e with the vertical line given by H (derived from Eq. 3, which includes frictional
 79 losses) indicates the global efficiency of the system. These zones are commented on below.

80 The lower limit adopted for excellent efficiency (zone A in Fig. 1) corresponds to a frequently
 81 used point: $I_e = 0.4 \text{ kWh m}^{-3}$; $H = 100 \text{ m}$ (ERSAR and LNEC, 2013). It corresponds to pumping
 82 100 m of height, with both ends at atmospheric pressure and a short pipe length. Therefore, $h_f \approx 0$,
 83 so $H \approx 100 \text{ m}$. Without leaks, this energy intensity corresponds to an overall pumping efficiency
 84 of 68%, which is a moderate value if current requirements are met (EC, 2012). Including leaks,
 85 this energy intensity corresponds, to a pumping efficiency of 75% and a water efficiency of 90%.
 86 The other zones are separated successively by 10 points in the efficiency product.



87

88 *Fig. 1. Assessment of the energy efficiency of a water transport system.*

89 Some final remarks apply:

- 90 a) The inclusion of head losses and pressure requirements in H (Fig. 1) is key to generalising
 91 the scope of Fig. 1. Graphs considering only the net elevation in the abscissa H (Plappally
 92 and Lienhard, 2012) are of more limited use.
- 93 b) In systems at the design phase, the real value of I_e is not yet known. In this case, using Fig.
 94 1, H can anticipate the range of energy intensities corresponding to different efficiencies.
 95 For the friction height, the value $h_f = J_o(L + \sum L_{ei})$ must be adopted, where J_o is the
 96 optimal hydraulic slope (Cabrera et al., 2018), and L and L_{ei} are the length of the system
 97 and the equivalent lengths of the accessories, respectively.
- 98 c) In simple systems, neither the pressure term, nor leakage inefficiencies, are usually
 99 involved.
- 100 d) The values of the parameter $\prod \eta_i$ are indicators that should reflect the evolution of
 101 technological improvements. For example, in submersible pumps, replacing asynchronous
 102 motors by synchronous ones improves the efficiency, especially at partial load (Sperlich et
 103 al., 2018). In short, in Fig. 1, the values of $\prod \eta_i$ must reflect the saving targets.
- 104 e) This assessment is based on the integral energy equation (a power balance) applied to
 105 systems limited by control-volumes (White, 1979), a balance that can be extended for any
 106 period of time. Therefore, any well-established system, no matter its size, can be assessed.
 107 Nevertheless, temporal variability of the system's efficiency can be analysed by extending
 108 the energy equation during the appropriate time interval, provided that for such period all
 109 the energy flows through the system's boundaries are known. In any case, for assessments
 110 of average energy, the focus of this paper, current time intervals (i.e. day, month or year)
 111 must be adopted.

112

113 Finally, and because friction is included as an additional requirement in H , it should be noted that
 114 Fig. 1 does not assess the system from the point of view of friction. Therefore, especially for
 115 systems in which friction is significant (e.g. where $h_f/H \geq 0.15$), its contribution must be evaluated
 116 independently. For this purpose, the friction efficiency, w_f , is of great interest and is defined as

$$w_f = \frac{h_f}{J_o(L + \sum L_{ei})}. \quad (5)$$

117

118 A w_f value different from 1 indicates that the diameter is insufficient ($w_f \gg 1$) or excessive ($w_f \rightarrow$
 119 0). The need for this complementary analysis increases with the length of the transport L and
 120 decreases with height. Obviously, if a facility is being designed, it is reasonable to design it with
 121 a diameter that corresponds to the optimal hydraulic slope, J_o , in which case, $w_f = 1$.

122

123 3. Different hydraulic grade lines

124 Regardless of whether the water transport is driven by gravity or pumped, the hydraulic slope J is
 125 a key parameter. In our analysis, four J parameters are defined:

- 126
- 127 ▪ J_{min} which corresponds to the lowest water speed. A minimum value is currently set to
 128 maintain quality (time of residence of the water in the system) and avoid sedimentation.
 - 129 ▪ J_o which corresponds to the optimal slope of a pipe requiring shaft energy. It is generally
 130 associated with pumping lines ($z_i < z_f$) but can easily be generalised to gravity pipes ($z_i >$
 z_f) in which the available slope $(z_i - z_f)/L$ is lower than J_{min} .

- 131 ▪ J_o^* which corresponds to the optimal slope of a gravity pipe in which some gravitational
 132 energy can be recovered. It is a similar concept to the previous one, but there are some
 133 differences. J_o is linked to the purchase price of the energy, whereas J_o^* is linked to the sale
 134 price (equations 7 and 8).
 135 ▪ J_{max} which corresponds to the maximum water speed. For the security of the facility (to
 136 control the water hammer) and the prevention of erosion, a given value should not be
 137 exceeded.

138 In general, $J_{min} < J_o < J_o^* < J_{max}$ applies, although systems with little use (i.e. low number of hours
 139 per year) can increase J_o to a value that is higher than J_{max} . In such a case, J_{max} is adopted. On the
 140 other hand, the optimal slopes, J_o and J_o^* , are incompatible (since one applies to pumped systems
 141 and the other applies to gravity systems, respectively). Lastly, the boundary values (J_{min} and J_{max})
 142 are subjective and depend on the reference consulted. Two examples follow.

- 143 a) According to the American Water Works Association (AWWA), J_{max} depends on the
 144 diameter. If it is less than 16 inches (≈ 400 mm), then $J_{max} = 7$ m km⁻¹. If this diameter is
 145 exceeded, then $J < 3$ m km⁻¹ (AWWA, 2012). Other authors (Bouman, 2014) have set the
 146 maximum water speed at 3 m s⁻¹; this is a very high value because for a 400 mm pipe (with
 147 a friction factor $f = 0.015$), $J \approx 17$ m km⁻¹. This value is unacceptable outside of exceptional
 148 cases (such as with a fire suppression network).
 149 b) The AWWA does not propose a value for J_{min} . It can be set from the minimum speed value
 150 of 0.2 m s⁻¹ (Bouman, 2014). For a diameter of 400 mm ($f = 0.020$), $J_{min} \approx 0.1$ m km⁻¹, a
 151 rather low value.

152 In short, under normal operating conditions, the interval (0.1 – 7) m km⁻¹ can be used as a reference,
 153 but singular cases require specific analysis. For instance, in penstocks of large hydroelectric plants,
 154 it is common to find speeds of up to 5 m s⁻¹ (Stevens and Davis, 1969), a value that is explained
 155 by short pipe lengths carrying very large flows.

156 The optimal slope comes from a well-defined expression that is shown in Eq. 6 (Cabrera et al.,
 157 2018). Its major uncertainty lies in the starting data since it is difficult to anticipate the average
 158 value of some of the equation's key parameters, such as the price of the energy, for a 50-year
 159 period (the pipe's expected lifespan). Its expression is

$$J_o = f_p \left(\frac{\lambda}{e} \right)^{\frac{5}{5+c}} \quad (6)$$

160 where f_p is dependent on the pipe parameters; c and λ lied on technical performance and cost,
 161 respectively, and e is a parameter that synthesises energy costs. Following Cabrera et al. (2018),
 162 the same equation can be expressed with additional parameters:

$$J_o = (0.0826 \cdot f)^{\frac{c}{5+c}} Q^{\frac{2c-5}{5+c}} \left[\frac{0.2c \cdot F_i \cdot a_o(p) \cdot \eta_p}{\gamma \cdot n \cdot h \cdot \bar{p}_e} \right]^{\frac{5}{5+c}} \quad (7)$$

163 where f is the friction factor, c and $a_o(p)$ are adjustment factors for pipe cost and diameter variation
 164 (very specific to the material), Q is the pipe flow, F_i is the installation factor (it includes all
 165 additional costs apart from the cost of the pipe itself: transport, trench, labour, etc.), η_p is the
 166 efficiency of the pumping station, γ is the specific water/fluid weight, h is the annual operating
 167 hours, and \bar{p}_e is the global average price of energy. Finally, it is important to underline that,
 168 because the constant 0.0826 has dimensions, Eq. 7 is not dimensionless (Cabrera et al., 2018) and
 169 requires application of SI units.

170 A gravitational pipe (as used for the penstock of a hydroelectric plant) is similar to a pumping line;
 171 therefore, the differences between J_o and J_o^* are minimal. In J_o , the energy term is quantified by
 172 the cost of the energy to be paid to the energy provider, $\overline{p_e}$; conversely, in J_o^* , the energy term is
 173 affected by the average selling energy price, $\overline{p_e^*}$. The second difference lies in η_p , the efficiency of
 174 the hydraulic machine (pump or turbine). In J_o , it appears in the numerator (the hydraulic energy
 175 is the output), while, in J_o^* , it is in the denominator (the hydraulic energy is an input). Thus, J_o^* is
 176 determined by

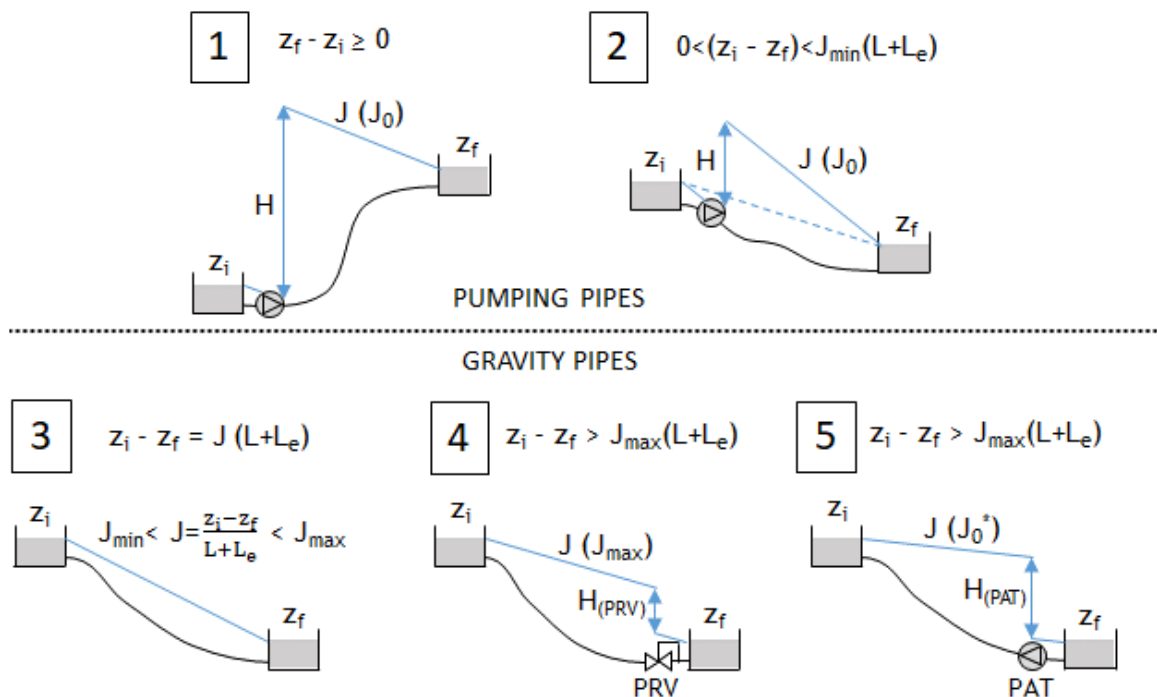
$$J_o^* = (0.0826 \cdot f)^{\frac{c}{5+c}} Q^{\frac{2c-5}{5+c}} \left[\frac{0.2c \cdot F_i \cdot a_o(p)}{\gamma \cdot n \cdot h \cdot \overline{p_e^*} \cdot \eta_t} \right]^{\frac{5}{5+c}} \quad (8)$$

177

178 4. Quick assessment of the energy efficiency of simple systems

179 As mentioned before, in the current context of climate change, it is necessary to generalise the
 180 energy analysis to all simple systems and not limit it to pumping systems. The possibility of
 181 recovering excess energy is arousing growing interest (Fecarotta et al., 2015). From this view,
 182 simple systems can be classified (Fig. 2) into five groups on the basis of energy.

- 183 1. Impulsion pipes (conventional pumping) must overcome elevation ($z_f - z_i \geq 0$) and friction.
 184 Shaft (pumping) energy, E_p , must be supplied.
- 185 2. Gravitational pipes ($z_f - z_i < 0$) have insufficient natural energy available because $(z_i - z_f)/L$
 186 $< J_{min}$. Therefore, additional shaft energy must be introduced.
- 187 3. Classic adduction means that the available natural energy can move the water at a
 188 reasonable speed.
- 189 4. Adduction with excess natural energy, ΔE , which energy cost analysis advises against
 190 recovering, means that the excess energy ($\Delta E = (z_i - z_f) - J_{max}L$) is dissipated with a PRV.
- 191 5. Adduction with excess, recoverable natural energy is a case similar to the previous one.
 192 However, the cost/benefit analysis is now positive.



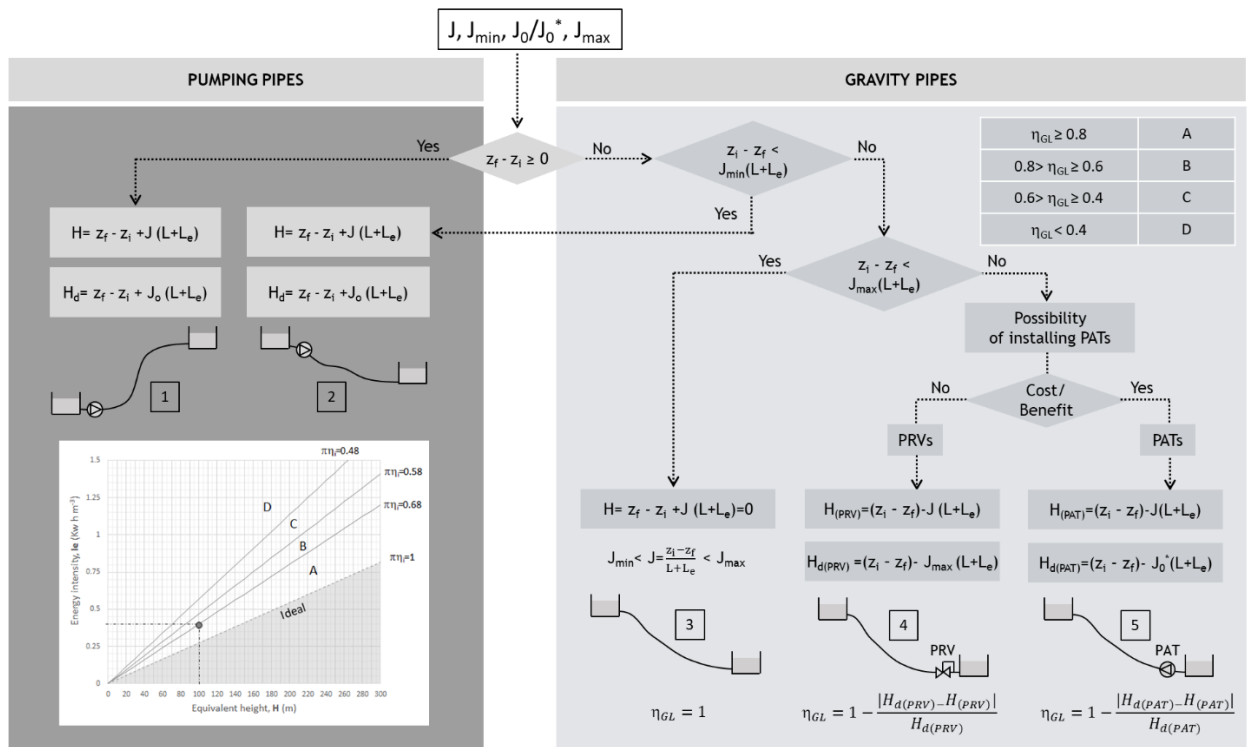
193

194 Fig. 2. Pressurised water transport in simple systems (different energy configurations).

195 Long-distance water transport systems include some (or all) of these five cases because the
 196 pipelines must be adapted to the topography of the terrain. Even if the slope of the terrain decreases
 197 monotonically (as in case 3), an open channel is a feasible solution. In any case, global energy
 198 analysis of the whole system must be performed in stages. Each section constitutes a volume of
 199 control to be analysed. Then, from the energy efficiency of each section and proper weighting, the
 200 final overall value is obtained. Notable examples of these transports are the California Aqueduct
 201 (CDWR, 2011), which is 700 km long with a $370 \text{ m}^3 \text{ s}^{-1}$ capacity; Israel's National Water Carrier
 202 (Cohen, 2008), which is 130 km long with a $20 \text{ m}^3 \text{ s}^{-1}$ capacity; and the Tajo Segura transfer system
 203 in Spain (Melgarejo and Montaña, 2009), which is 290 km long with a $33 \text{ m}^3 \text{ s}^{-1}$ capacity.

204 Figure 3 qualifies each case from an energy perspective. The process begins with the calculation
 205 of hydraulic slopes. The order of magnitude of the extremes (J_{min} and J_{max}), although subjective,
 206 is well defined, while J_o and J_o^* must be calculated appropriately. For operational pumping pipes
 207 (left column, cases 1 and 2), if the system is working, the adopted hydraulic slope is the real one,
 208 J . H is determined from J , and the efficiency is obtained. During the design phase of pipelines,
 209 the goal is to set the intervals of I_e that correspond to each efficiency level. These ranges are
 210 established by means of J_o and H_d (the d subscripts refer to the design phase).

211 The qualification of gravitational adductions (cases 3, 4, and 5) is, to some extent, subjective.
 212 Natural energy therefore has no cost and minimising costs is futile. However, I_e , the basic indicator
 213 of the analysis and linked to the energy to be paid, does not exist. It only makes sense in adductions
 214 with PATs, which is a case of economic balance in the conventional context. In case 3, in which J
 215 lies between the extreme slopes, there is no alternative and, therefore, the global efficiency (η_{GL})
 216 is equal to 1. In cases 4 and 5, the measure of efficiency is linked to the difference between the
 217 real H and the designed one, H_d .



218

219

220

Fig. 3. Energy efficiency of pressurised water transport in simple pipelines.

221 5. Quick assessment of the energy inefficiencies in networks: operational and structural 222 losses

223 The assessment of the energy efficiency of complex systems resembles that of simple systems,
224 although there are important differences. The first and most relevant one is the existence of
225 topographic energy, which is a consequence of different consumption at different heights (in
226 simple systems, there is just one delivery point). The design of any network aims to meet the
227 requirements of the most unfavourable node, while the volume of the other nodes is delivered with
228 excess pressure (the higher the node, the lower the pressure). The sum of all these excesses is
229 topographic energy, E_{ti} (Cabrera et al., 2015). This energy is not an energy loss linked to the
230 system's operation, although, in practice, it implies that more energy is supplied than is strictly
231 necessary. Therefore, it is advisable to associate that energy with another type of inefficiency, that
232 is structural loss (Cabrera et al., 2019). The second difference is the potential presence of several
233 energy sources. In a network, it is common to supply water from two (or more) pumping stations
234 or reservoirs.

235 Once the system is defined (with its surface and volume of control), the integral energy equation
236 can be applied (Cabrera et al., 2010b). For this reason, in complex systems, it is common to divide
237 the supplied (or injected) energy (E_I) into natural (E_N) and pumping energy (E_p): $E_I = E_N + E_p$. The
238 weight of each form is represented by the parameter $C_I = E_N/(E_N + E_p) = E_N/E_I$. In simple systems,
239 the energy injected, E_I , only has both components in scenario 2.

240 There remains a third major difference between simple and complex systems. It is possible to
241 define the optimal hydraulic slope, J_o , in both types (Cabrera et al., 2018). Nevertheless, this is not
242 the case for the slope J_o^* , which is typical of simple gravitational systems. The explanation is clear:
243 while J_o is based on the evaluation of the friction in all pipes, it is unrealistic to assess the energy
244 in any line in which it could be recovered with PATs, and this is the basis of J_o^* . So, it is a challenge
245 to typify complex networks the way that simple systems are characterised in Fig. 3. There are
246 additional minor differences, such as the habitual existence of leaks in complex systems (in simple
247 systems, they are usually negligible) or the current requirement to supply pressure of service p_o in
248 networks.

249 Despite these differences, calculating the energy efficiency of a network is similar to that of a
250 simple system. However, in this new case, the starting point is the minimum energy E_{si} required
251 by the system for a period of time T. This energy can be expressed (Cabrera et al., 2015) by

$$E_{si} = \gamma V \left[(z_h - z_l) + \frac{p_o}{\gamma} \right] \quad (9)$$

252 where γ is the specific weight of the water (N m^{-3}), V is the volume supplied (m^3) to the system in
253 period T, z_h and z_l are the elevation (m) of the extreme (highest and lowest) nodes and p_o is the
254 pressure of service (N m^{-2}). To this minimum energy, the energy required to overcome friction
255 must be added. This term is more diffuse in water-looped networks than in simple systems because
256 the water path is not a priori defined. To overcome this problem, the friction energy is maximised,
257 adopting the energy lost between the source and the critical node for the whole system. In a real
258 network, this value can be measured or, alternatively, estimated by multiplying the distance
259 between the two points (L) by a reasonable hydraulic grade line slope; for instance, $J = 0.0015$
260 m/m. In a real case, if J is ultimately higher than the estimated value, H will be smaller.
261 Consequently, the energetic requirements of the system will be smaller, too.

262 In short, assuming that the suction pressure is zero, the equivalent final height H , with the real h_f
 263 measured (the abscissa of Fig. 1), is determined by

$$H = (z_h - z_l) + \frac{p_o}{\gamma} + h_f. \quad (10)$$

A quicker but less accurate estimation (without measurements) is obtained from

$$H = (z_h - z_l) + \frac{p_o}{\gamma} + 0.0015 \cdot L. \quad (11)$$

264 In Fig. 1, the purpose of the intersection between the horizontal given by I_e and the vertical defined
 265 by H (equation 10 or 11) is to qualify the behaviour of the system in terms of energy and, at the
 266 same time, determine the margin for improvement. The relevance of the friction, h_f/H , which is
 267 typically moderate in networks, indicates whether the estimation's error is more or less significant.

268 Finally, if the height of the source, z_s , is intermediate between extremes ($z_l < z_s < z_h$), natural energy
 269 must be included in the balance. The natural energy is

$$E_N = \gamma V(z_i - z_l). \quad (12)$$

270 The natural energy plus the shaft energy amounts to the total energy injected, E_I . The result
 271 obtained from Figure 1 illustrates the overall energy assessment of the network and includes both
 272 operational and structural losses. This is because the energy requirements were calculated
 273 according to the needs of the most unfavourable node.

274 In order to assess the contribution of structural losses to the inefficiency, it is necessary to calculate
 275 the weight of the topographic energy, E_{ti} , relative to the total energy requirements. In a network
 276 without friction (Cabrera et al., 2015), topographic energy is equal to

$$E_{ti} = \gamma \sum v_j [(z_h - z_j)] \approx \gamma V(z_h - \bar{z}) \quad (13)$$

277 where v_j is the water consumption of node j , z_j is its height and \bar{z} is the weighted average of the
 278 consumption nodes. In Eq. 13, E_{ti} can be roughly estimated from the extreme nodes' average
 279 elevation. This approach is reliable for uniform spatial demand distribution. However, if most of
 280 the consumption transpires in the upper part of the network, the average value overestimates E_{ti} ;
 281 in the opposite case, E_{ti} is underestimated. As previously mentioned, the topographic energy is the
 282 total excess of the energy delivered, and it is independent of the type of energy (natural or pumped).
 283 The relation between E_{ti} and the ideal total energy delivered is the parameter θ , the weight of
 284 structural losses in the energy balance. That is,

$$\theta = \frac{\sum v_j [(z_h - z_j)]}{V [(z_h - z_l) + \frac{p_o}{\gamma}]} \quad (14)$$

285 The value of θ enables the decoupling of the total energy losses and, therefore, the identification
 286 of the most effective improvement strategies. Better management reduces the operational losses,
 287 while structural losses can only be diminished with a layout modification (Cabrera et al., 2019).

288

289

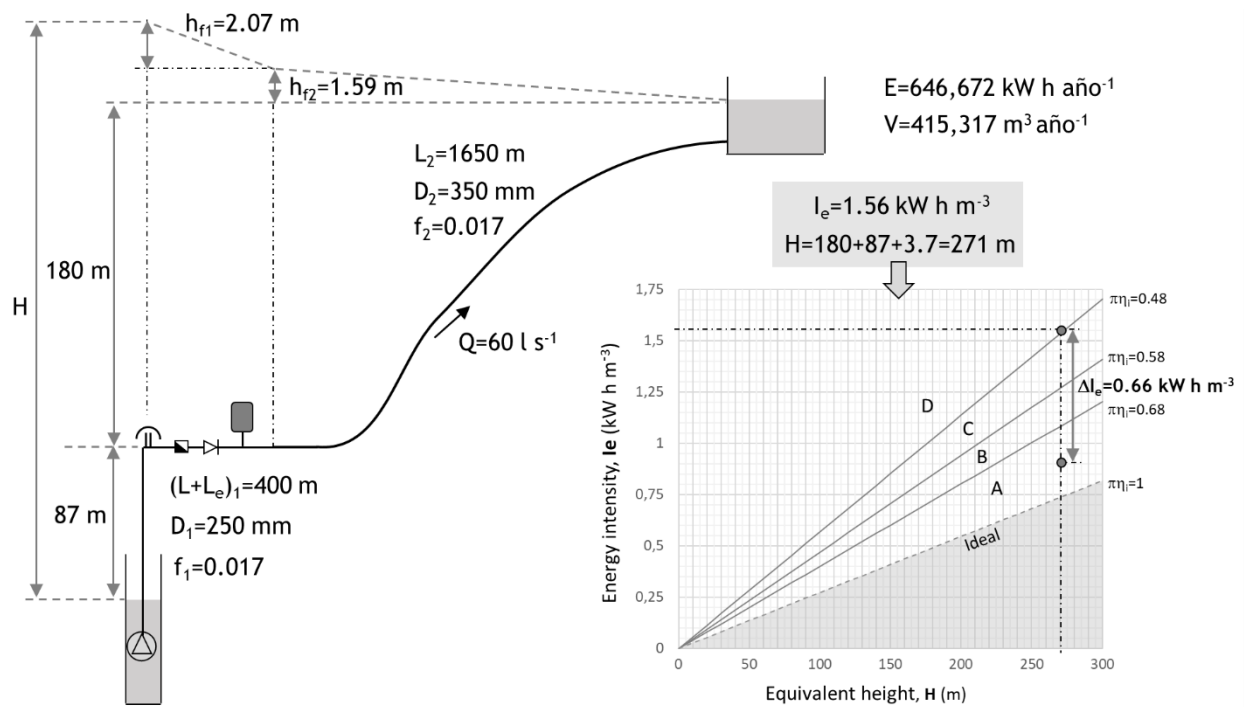
290

291 **6. Examples**

292 Three examples are presented to clarify the concepts previously explained. Two of them are in
 293 operation (Examples 1 and 3). Example 2 is in the design phase: specifically, it describes a working
 294 facility that is being renovated. The objective in each example is to assess their energy efficiency
 295 behaviour.

296 **6.1. Example 1. Pumping line**

297 Water is pumped from a well to a tank (Fig. 4). The use is residential (25%) and agricultural (75%);
 298 therefore, the number of hours of operation per year is variable. In 2018, the total energy
 299 consumption was 646672 kW h, and 415317 m³ was pumped ($I_e = 1.56 \text{ kW h m}^{-3}$).



300

301 *Fig. 4. Simple pipeline in Castellon (Spain) with its energy assessment.*

302 The equivalent height H (270.66 m) is equal to the water elevation (267 m) plus friction losses h_f
 303 (3.66 m). The defined lines meet at a point located in the unsatisfactory–unacceptable zones (zones
 304 C-D in Fig. 4), and there is considerable room for improvement before reaching a status of
 305 excellent (0.66 kW h m^{-3} , greater than 40%). This justifies a thorough review of the system’s
 306 operation. In the absence of leaks, the conclusion is obvious: all operational inefficiencies are
 307 located at the pumping station, with a global efficiency of 49% (Fig. 4). However, seasonal
 308 variations in the well water table level can contribute to this degree of poor performance.

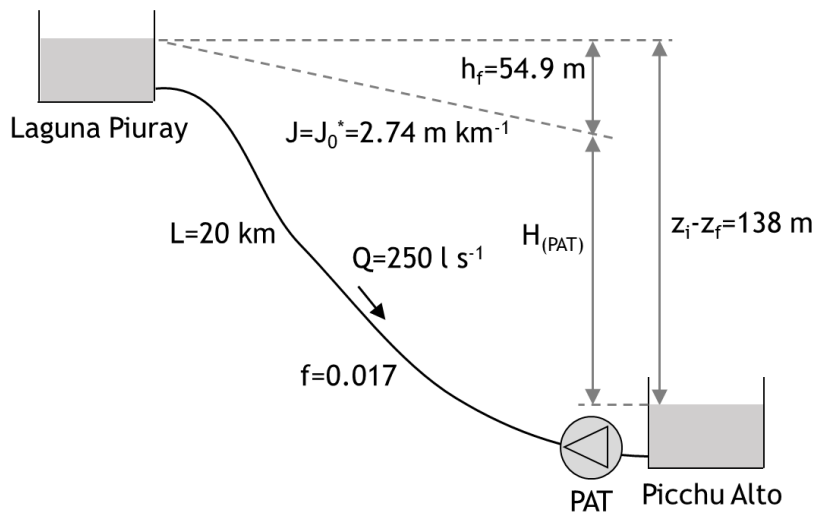
309 Figure 1 does not assess the contribution of friction. That is, it does not answer the question of
 310 whether 3.66 m of friction is (or is not) a reasonable value. To this end, the first step is to calculate
 311 J_o (equation 7). The basic data of a cast iron pipe are $c = 1.4$; $a_o(p) = 635.575 \text{ € (m} \cdot \text{m}^{1.4})^{-1}$; $n = 50$
 312 years; $F_i = 1.5$; $\bar{p}_e = 0.14 \text{ € kW h}^{-1}$; $h = 4000 \text{ h year}^{-1}$ and $\eta_p = 75\%$, which is a more reasonable
 313 pump efficiency than the current value (49%). These data should represent the pipe’s 50-year
 314 average lifespan. From these values, $J_o = 2,213 \text{ m km}^{-1}$, and the optimal head loss is 4.56 m ($L_T =$
 315 2.05 km), which is almost equal to the actual value (3.66 m). In short, $w_f = 3.66/4.56 = 0.80$, while
 316 the weight of friction is low ($h_f/H = 3.66/270.66 = 0.014$), and it should be less without the

317 contribution of local losses (e.g. foot valves, filters, elbows, etc.). Therefore, system's friction is
 318 reasonable.

319

320 6.2. Example 2. Gravity line

321 This example corresponds to an operational gravity pipe in Cusco, Peru (Fig. 5). The old pipeline
 322 requires renewal and, at the same time, the potential recovery of excess gravitational energy
 323 (actually dissipated by a PRV located at the entrance to the Picchu Alto tank) is economically
 324 feasible. For the new cast iron pipe, data from Example 1 are assumed to apply. The specific data
 325 are $F_i = 1.5$; $\bar{p}_e^* = 0.08 \text{ € (kW h)}^{-1}$, $h = 8760 \text{ h year}^{-1}$ and PAT efficiency = 72%. From these data,
 326 J_o^* (equation 8) is $2,743 \text{ m km}^{-1}$, which corresponds to a 502 mm diameter pipe (rounded to 500
 327 mm). The energy to be recovered by the PAT (H_{PAT}) should be 83.1 m. A positive cost/benefit
 328 analysis would justify its installation. As seen in Figure 5, the energy efficiency of the design
 329 would be the unit.



$\eta_{GL} \geq 0.8$	A
$0.8 > \eta_{GL} \geq 0.6$	B
$0.6 > \eta_{GL} \geq 0.4$	C
$\eta_{GL} < 0.4$	D

$$\eta_{GL} = 1 - \frac{|H_{d(PAT)} - H_{(PAT)}|}{H_{d(PAT)}}$$

$$\eta_{GL} = 1 - \frac{|83.1 - 83.1|}{83.1} = 1$$

330

331 *Figure 5. Gravity pipeline in Cusco (Peru).*

332 6.3. Example 3. Irrigation network

333 In 2011, the irrigation network shown in Figure 6 displayed poor energy-related behaviour.
 334 Operational data for an average day in that year were an injected flow of $19164 \text{ m}^3 \text{ d}^{-1}$, supplied
 335 flow of $18580 \text{ m}^3 \text{ d}^{-1}$ (leaks = $584 \text{ m}^3 \text{ d}^{-1}$, a good performance for a 5-year-old network), pressure
 336 service of 20 m and consumed shaft energy of 5833 kW h d^{-1} . The physical data are $z_h = 35.53 \text{ m}$,
 337 $z_l = 14.39 \text{ m}$ and the suction pressure, z_s , 25.00 m. The length from the source to the most
 338 unfavourable node is 3 km (the total network length is slightly over 50 km).

339

340 From these data, $H \approx (35.53 - 14.39) + 20 + 0.0015 \cdot 3000 = 45.64 \text{ m}$. The energy intensity, I_e ,
 341 (considering the natural energy of 554 kW h) is

342

$$343 I_e = \frac{5833 + 554}{18580} = 0.34 \text{ kWh m}^{-3}.$$

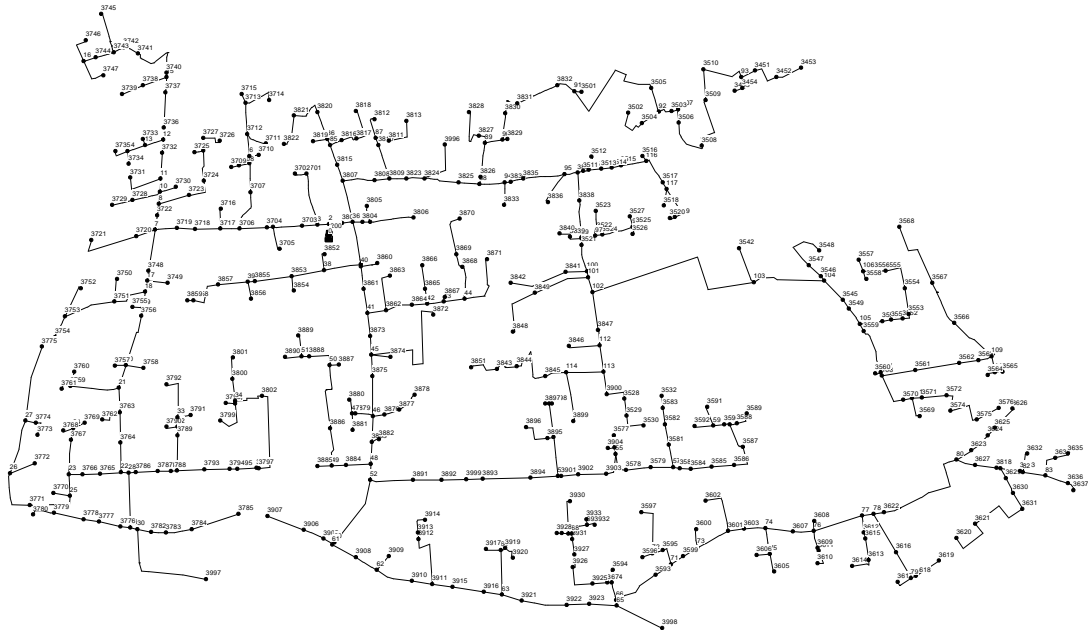


Figure 6. Irrigation network in Vila-Real (Spain).

This point (45.64; 0.34) falls into the D (unacceptable) area (Fig. 1), given that this energy evaluation of the network occurred before any improvement. In order to assess the weight of the structural losses, the topographic energy was estimated by Eq. 13. The result is

$$E_{ti} \approx \gamma \cdot V(z_h - \bar{z}) = 9810 \cdot 19164 \cdot \left(35,54 - \frac{35,54+14,39}{2}\right) = 1,99 \cdot 10^9 \text{ J d}^{-1} = 552,78 \text{ kW h d}^{-1}.$$

In this case, the correct topographic energy (588.71 kW h d⁻¹), evaluated using the non-simplified Eq. 13, is slightly higher than the approximated value (552.78 kW h d⁻¹), a small difference due to the relatively homogeneous spatial distribution of the demand.

If the inefficiencies are only due to operational losses, I_e is recalculated without considering the topographic energy; the result is $I_e = 0.31 \text{ kW h m}^{-3}$. This value intersects with $H = 45.64 \text{ m}$ in Figure 1 and again results in an unacceptable assessment (D zone). This figure shows that the network efficiency should only be classified as excellent if $I_e < 0.17 \text{ kW h m}^{-3}$. After some operational and structural improvements, the present energy intensity is 0.16 kW h m^{-3} . As the focus of this paper is on the average values only a brief description of the three main implemented actions (one operational and two structural) are provided:

- a) This system operated with two turns of two hours each with rigid patterns for irrigation and very different flows (up to 50% of difference). With that variability, the system could hardly operate constantly at best efficient point (BEP). The irrigation was re-scheduled (constant flow, no matter the turn) and with these new load conditions, one of the five pumps was stopped, and the remaining operating pumps worked steadily at their BEP.
- b) Local losses at the pumping and filtering station were very high (10 m). With a more rational piping layout and new efficient filters, this loss was dramatically reduced (3 m).
- c) The pumps, working in parallel, supplied water to the highest and lowest nodes. To reduce the topographic energy, the network was divided into three independent sectors and the pumps were conveniently decoupled. Although the partition, strongly conditioned by the existing network, was not the optimum, the requested energy by the four pumps was significantly reduced.

378 7. Conclusion

379 A methodology designed to perform quick energy assessments for irrigation water transport
380 systems is presented. Among these systems, those that require pumping energy are of special
381 interest because of their economic implications. The proposed procedure is based on the fact that
382 the energy intensity units (kW h m^{-3}) are effectively pressure units as well (N m^{-2}). Therefore, a
383 direct and biunivocal relationship between I_e and the equivalent height H (sum of the energies
384 required per unit of weight) can be established. From the real transport needs (I_e) and the minimum
385 energy needs (H), the inefficiencies (in kW h m^{-3}) can be estimated. This analysis requires use of
386 concepts that are generally ignored, such as natural energy or topographic energy.

387 From the physics of pressurised water transport systems, with the inefficiencies duly classified (as
388 operational losses, pumps and leaks, and friction) and quantified, the global efficiency can be
389 assessed. The proposed labels (Fig. 1) are, to some extent, subjective and can be reformulated from
390 the energy efficiency goals set by the regulators and the current state of the technology.

391

392 REFERENCES

393 AWWA, American Water Works Association. (2012). Computer Modeling of Water Distribution
394 Systems. *AWWA Manual M32. Third Edition*. Denver. Colorado. USA.

395 Bouman, D. (2014). Hydraulic design for gravity based water schemes. *Aqua for All*. Den Haag.
396 The Netherlands.

397 Cabrera, E., Pardo, M., Cabrera, E. Jr., & Cobacho, R. (2010a). Agua y Energía en España. Un
398 reto complejo y fascinante. *Ingeniería del Agua*, (17-3), 235-246.

399 Cabrera, E., Pardo, M., Cobacho, R., & Cabrera, E. Jr. (2010b) Energy audit of water networks.
400 *Journal of Water Resources Planning and Management*, 136, 669-677.

401 Cabrera, E., Gómez, E., Cabrera, E. Jr., Soriano, J., & Espert, V. (2015). Energy assessment of
402 pressurized water systems. *Journal of Water Resources Planning and Management*. DOI:
403 10.1061/(ASCE)WR.1943-5452.0000494.

404 Cabrera, E., Gómez, E., Cabrera, E. Jr., & Soriano, J. (2018). Calculating the economic level of
405 friction in pressurized water systems. *Water* 2018, 9, 763. DOI: 103390/w10060763.

406 Cabrera, E., Gómez, E., Soriano, J., & del Teso, R. (2019). Eco-layouts in water distribution
407 networks. *Journal of Water Resource Planning Management*, 2019, 145(1): 04018088. DOI:
408 10.1061/(ASCE) WR.1943-5452.0001024.

409 CDWR, California Department of Water Resources. (2011). *California State Water Project at a*
410 *glance*. Department of Water Resources. State of California, USA April 2011.

411

412 Cohen, N. (2008). Israel's National Water Carrier. *Present environment and sustainable*
413 *development, Volume 2, Issue 1, 15-27*.

414

415 EC, European Commission. (2011). *Directive of the European Parliament and of the Council on*
416 *energy efficiency and repealing Directives 2004/8/EC and 2006/32/EC*. Brussels, 22.6.2011 COM
417 (2011) 370 final.

418

419 EC, European Commission. (2012). *Directive 2009/125/EC of the European Parliament and of*
420 *the Council with Regard to Ecodesign Requirements for Water Pumps*. Official Journal of the
421 European Union. 26.6.201.
422

423 EC, European Commission. (2019). *Fourth Report on the State of the Energy Union*. Brussels,
424 9.4.2019 COM (2019) 175 final.
425

426 ERSAR & LNEC. (2013). *Guide to the quality of service assessment for drinking water supply,*
427 *urban wastewater management and municipal waste management services - 2nd generation of the*
428 *assessment system (in Portuguese)*. 2nd ed. Lisbon: ERSAR.
429

430 Fecarotta, O., Aricò, C., Carravetta, A., Martino, R., & Ramos, H. M. (2015). Hydropower
431 Potential in Water Distribution Networks: Pressure Control by PATs. *Water Resources*
432 *Management* 29:699–714. DOI 10.1007/s11269-014-0836-3.
433

434 Ghorbanian, G., Karney, K., & Guo, Y. (2016). Pressure Standards in Water Distribution Systems:
435 Reflection on Current Practice with Consideration of Some Unresolved Issues. *Journal of Water*
436 *Resources Planning and Management*. ASCE. DOI: 10.1061 / (ASCE) WR. 1943 - 5452.0000665.

437 Grundfos. (2014). *High efficiency motor technology that reduces energy waste in pump*
438 *applications*. Grundfos. Denmark.

439 Melgarejo, J. & Montaña, B. (2009). La eficiencia energética del trasvase Tajo-Segura.
440 *Cuaderno Interdisciplinar de Desarrollo Sostenible*, CUIDES, nº 3.
441

442 Plappally, J. H. & Lienhard, V. J. H. (2012). Energy requirements for water production, treatment,
443 end use, reclamation, and disposal. *Renewable and Sustainable Energy Reviews* 16 (2012) 4818–
444 4848.

445 Sperlich, A., Pfeiffer, D., Burgschweiger, J., Campbell, E., Beck, M., Gnirss, R., & Ernst, M.,
446 (2018). *Energy Efficient Operation of Variable Speed Submersible Pumps: Simulation of a Ground*
447 *Water Well Field*. *Water* 2018, 10, 1255.

448 Stevens, J. C. & Davis, C. V. (1969). *Hydroelectric Plants*. Section 24 of the Handbook of Applied
449 Hydraulics. Edited by Calvin Victor Davis and Kenneth E. Sorensen. Mc Graw Hill. New York.

450 White, F. M. (1979). *Fluid Mechanics*, McGraw-Hill, Inc.: New York. ISBN 10: 0070696675.

451 WW, Water in the West. (2013). *Water and Energy Nexus: A Literature Review*. Stanford
452 University, CA, USA.
453
454